Effects of Interfacial Specific Cation and Water Molarities on AOT Micelle-to-Vesicle Transitions by Chemical Trapping: The Specific Ion-Pair/Hydration Model

Journal:	*Physical Chemistry Chemical Physics*
Manuscript ID	CP-ART-09-2018-005987.R2
Article Type:	Paper
Date Submitted by the Author:	12-Feb-2019
Complete List of Authors:	Liu, Changyao; Beijing Technology and Business University, School of Food and Chemical Engineering Wang, Yuzhao; Beijing Technology and Business University, School of Food and Chemical Engineering Gao, Yanfei; Beijing Technology and Business University, School of Food and Chemical Engineering Zhang, Yongliang; The State University of New Jersey, Chemistry and Chemical Biology Zhao, Li; Beijing Technology and Business University, School of Food and Chemical Engineering Xu, Baocai ; Beijing Technology and Business University, School of Food and Chemical Engineering Romsted, Laurence; The State University of New Jersey, Chemistry and Chemical Biology

Effects of Interfacial Specific Cation and Water Molarities on AOT Micelle-to-Vesicle Transitions by Chemical Trapping: The Specific Ion-Pair/Hydration Model

Changyao Liu,[1] Yuzhao Wang,[1] Yanfei Gao,[1] Yongliang Zhang,[2] Li Zhao,[1] Baocai Xu,*[1] and Laurence S. Romsted*[2]

[1]School of Food and Chemical Engineering, Beijing Technology and Business University, No. 11 Fucheng Road, Beijing, 100048, People's Republic of China

[2]Department of Chemistry and Chemical Biology, Rutgers, The State University of New Jersey 610 Taylor Road Piscataway, New Jersey 08854

Abstract

Salt induced micelle-to-vesicle transitions of ionic surfactants depend on surfactant chain length, headgroup structure, counterion type and concentration, but the interfacial molarities of counterions and water that balance the hydrophobic effect are difficult to determine. In anionic micelles of twin-tailed sodium bis (2-ethylhexyl)sulfosuccinate (AOT), the chemical trapping (CT) method provides estimates of the interfacial molarities of anionic headgroups ($RSO_3^-{}_m$) and neutral (H_2O_m) nucleophiles during salt induced transitions of AOT micelles to vesicles. Product yields were measured by HPLC from the competitive dediazoniation reaction using a specially designed hydrophobic probe, 4-hexadecyl-2,6-dimethylbenzenediazonium cation, 16-ArN_2^+. The reactions were run at constant, 15 mM AOT mixed with 0 to 50 mM added salts, containing cations of different sizes and valences including tetraalkylammonium cations (MR_4^+, R = 1-4) and metal cations ($M^{1\text{-}3+}$). Parallel reactions in aqueous salt solutions with a short chain analog, 1-ArN_2^+, were used as references to calculate interfacial molarities. Aggregates were structurally characterized by TEM and DLS. Typically, interfacial RSO_3^- molarities increase with added salt from 1 to 2 M and water molarities decrease from about 40 to 20 M as the micelles transition to vesicles. These changes are consistent with the Ion-Pair/Hydration model, in which the added cations form neutral but polar ion-pairs with RSO_3^- that had a lower demand for hydration and water was released into the surrounding aqueous phase. The extent of ion-pairing increases with cation size, charge and hydrophobicity and decreases in interfacial water molarity, which permits tighter interfacial packing and vesicle formation at lower added salt concentrations.

Introduction

Micelle-to-vesicle and other structural transitions of ionic surfactants are widely reported and generally depend on a number of variables such as surfactant chain length, headgroup structure, nature of the counterion and the concentration of surfactant and added salt.[1-4] However, the specific forces responsible for interactions in the interfacial regions of micelles are difficult to determine quantitatively.[5, 6] For example, vesicles form spontaneously in micellar solutions when the surfactant concentration of twin-tail surfactants, e.g., phospholipids with appropriate chain lengths, are increased[7]

or salts[8] are added. The surfactant headgroups are generally arrayed at the interior, endo, and exterior, exo, vesicular surfaces and their terminal methyls are oriented in the fluid interior between the tails in a closed spherical or ellipsoidal unilamellar vesicles (ULV) or in concentric layers in multilamellar vesicles (MLV).[9] Hofmeister first reported ion specific effects on protein solubilities in the late 1800s.[10-19] Since then ion-specific effects have been reported on the solution properties of ionic colloids, biomembranes and proteins[20-22] and these aggregates are used as cell membrane models,[23, 24] microreactors, nanotemplates and drug carriers.[25-29]

Specific effects are generally attributed to specific headgroup-counterion pairing and contributing interactions discussed earlier. These interactions have been studied in greater detail in recent experimental and theoretical work.[6, 30-38] For a series of counterions to a single chain ionic surfactant headgroups, specific ion effects often follow similar orders and correlated with a variety of counterion properties. Sometimes separate orders are reported for anions and cations. Aggregate properties that are affected by counterion type include the critical micelle concentration (cmc), Krafft temperature, ionization degree, micellar effects on rates of first and second order reactions, and indicator pK_as.[39-41] Sometimes the dependence on counterion type is large. Kunz et al. reported that micelle-to-vesicle transitions in multiple catanionic surfactant solutions are sensitive to added alkali cations, and Salis and others reported specific cation effects on hemoglobin aggregation.[42] The critical salt concentrations (CSCs) may also depend on headgroup structure, e.g., sulfate or carboxylate headgroups, follow the direct and reverse Hofmeister series respectively.[43-47] Mixtures of oppositely charged single-tail surfactants such as cetyltrimethylammonium tosylate and sodium dodecyl benzene sulfonate,[48] dodecyltrimethylammonium bromide and sodium dodecyl sulfate,[49] and cetyltrimethylammonium bromide and sodium octyl sulfate form vesicles at well-defined ratios of the two surfactants.[7, 50]

The balance-of-forces in the interfacial regions within micelles are delicate, and one important factor is the counterion-headgroup interactions that are difficult to determine experimentally.[38] The twin-tailed sodium bis(2-ethylhexyl)sulfosuccinate (AOT) is a well-studied surfactant because it readily forms reverse micelles in organic solvents containing small amounts of water.[51, 52] Less well studied are the properties of aqueous solutions of AOT that undergo micelle-to-vesicle transitions with added salts,

e.g. NaCl, NaBr, KCl, KBr, and organic sodium salts.[33, 53-56] Ismail and coworkers also reported surface tension, fluorescence, small angle neutron scattering, and dynamic light scattering measurements below and above the CSCs for micelle-to-vesicle transitions in aqueous AOT solutions, including added tetraalkylammonium bromide (TAABr) salts, where alkyl = ethyl (TEABr), propyl (TPABr) and butyl (TBABr)), and the effect of NH_4Cl.[8, 33, 41, 57, 58]

We have used the CT method to study specific salt effects on aqueous AOT micelles because the method had not been previously used with an anionic surfactant, and because Ismail's group recently reported interesting specific cation effects on a range of AOT properties through the CSC transition, i.e., from below to above the micelle-to-vesicle transitions. As shown in the Results and Discussion section, CT reports on the change in interfacial molarities in units of moles per liter of interfacial volume (indicated by a subscripted m) of RSO_3^- headgroups, AOT_m, and H_2O_m in AOT solutions with added MCl salts with different cations. The results show that the micelle-to-vesicle transitions are clearly sensitive to changes in cation type, but insensitive to anion type because no product was formed between 16-ArN_2^+ and different co-ions of added salts, just RSO_3^- and H_2O products both in significant yields.

Applying the Chemical Trapping Method to AOT Salt Solutions

Important Operational Assumptions. We make three assumptions when using the CT method: (a) The Pseudophase Model Works. The AOT/salt solutions are homogeneous and optically transparent, the surfactant aggregates can be treated as separate pseudophases composed of aqueous, interfacial and hydrocarbon core regions; (b) All components in the surfactant solutions are in dynamic equilibrium, i.e., their molecular diffusivities are orders of magnitude faster than the dediazoniation reaction or other bulk physical measurements; and (c) The totality of the interfacial regions of all the aggregates in solution form an interfacial pseudophase. Mathematical models used to treat of rates and equilibria begin with these pseudophases and are not needed in the CT method because neither rate nor equilibrium constants are measured, only product yields.[59-61]

The Chemical Trapping (CT) Method. The CT method was developed by our group[62] and others in Brazil[63] and India[64] over a number of years to determine the interfacial molarities of weakly basic anionic and neutral nucleophiles, including water, in association colloid solutions.[62, 65, 66] The CT method

was recently reviewed.[67, 68] Product yields from the spontaneous heterolytic dediazoniation of an amphiphilic, but hydrophobic arenediazonium ion, 4-hexadecyl-2,6-dimethylarenediazonium ion, 16-ArN_2^+, prepared as its BF_4^- salt, is very soluble in association colloids. Product yields in the association colloids are converted to interfacial molarities by using product yields from reaction of the short chain analog, 1-ArN_2^+, in aqueous solutions containing the same nucleophiles, but with short-chain nonmicellizing headgroup models to determine the selectivity of the reaction with the headgroup model relative to water.[69] Previous CT measurements with micelles of ionic surfactants that undergo sphere-to-rod transitions occur with a concomitant increase of interfacial counterion and a decrease of interfacial water molarities.[70] Our results here are completely consistent with these observations.

Logic of the CT Method. 16-ArN_2^+ in micellar solutions and 1-ArN_2^+ in aqueous reference solutions react competitively and by the same mechanism with water molecules and the RSO_3^- headgroups of AOT, **Figure 1**. Note: sulfonic acids are strong acids, pK_a < -1.9,[71] and will be completely deprotonated under our experiments at 1 mM acid added to control solution pH. The same reactions occur between the 1-ArN_2^+, and water and a short chain AOT headgroup analog, sodium dimethylsulfosuccinate (SDSS), in aqueous solutions. The trapping of 1-ArN_2^+ by water and the AOT sulfonate headgroup (and SDSS) were determined previously.[64] The yields of products, z-ArOH and z-ArS, are measured by HPLC. These yields are used to estimate their interfacial molarities from product yields from 16-ArN_2^+ by assuming that when the aqueous and interfacial product yields are the same, their molarities and the selectivities of the reaction are the same. **Figure 2** illustrates this idea. When the yields from reaction of 16-ArN_2^+ with AOT and H_2O within interfacial pseudophase **(Figure 2A**, green region) are the same as the yields from reaction of 1-ArN_2^+ with the SDSS, (**Figure 2B**) and water, then the molarities of H_2O_m and RSO_3^-

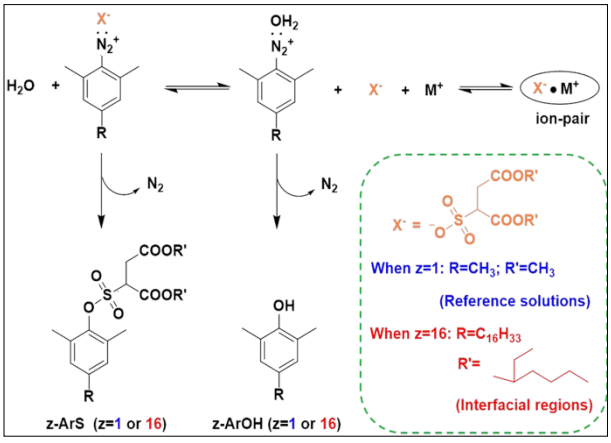

Figure 1. Ground state dynamic equilibria in the interfacial region of aggregates between water, AOT headgroup, X^-, and long-chain arenediazonium ion, z = 16, R = $C_{16}H_{33}$, or in aqueous SDSS (R' = CH_3) reference solution in the absence of aggregates with short-chain arenediazonium ion, z = 1, R = CH_3. A fraction of AOT headgroups (R = -$C_{16}H_{33}$) or their analogs (R = -CH_3) and form ion-pairs with cations, M^+, in both regions.

$_m$ are the same in the micellar interfacial region and in the aqueous reference solution. Put differently, we assume that the selectivity of the dediazoniation reaction toward water and RSO_3^- in the interfacial region and water are the same when product yields of AOT headgroups and H_2O within the interfacial region are the same as those with SDSS and H_2O in an aqueous reference solution, **Figure 2**. Thus, the interfacial molarities are the same in the aqueous reference solution when the product yields are the same in both regions. Details on determining the interfacial molarities are in the **Experimental Section**.

Results and Discussion

Dynamic Light Scattering (DLS) Results. **Table 1** lists the mean diameter in nanometers, nm, and standard deviations for triplicate DLS measurements for each salt used in the CT experiments. These results will be compared with the CT results below. The DLS measurements were made at 50 mM salt or the maximum salt concentrations obtainable in a particular CT experiment (see **Experimental Section**). Careful inspection shows that at 50 mM salt, a majority of the aggregates have mean diameters on the order of 70-110 nm. The mean diameters of TEABr and TPABr cations at 50 mM added salt are >200 nm, larger than those of TMABr. TBABr aggregates are even larger, ca. 10^3 nm, at 30 mM. The solution separates at higher concentrations. Ca^{2+} and Al^{3+} form aggregates >200 nm at 7 mM salt and precipitate at higher concentrations. Additional details are discussed with **Figures 3, 4**, and **6**.

Figure 2. Box **A** is a small section of the immediate vicinity of the interfacial region of an AOT micelle or vesicle in aqueous solution in which long-chain probe, 16-ArN_2^+, is trapped by water (not shown) and AOT headgroups. Box **B** is a portion of the aqueous reference solution in which short-chain probe, 1-ArN_2^+, is trapped by water (not shown) and the AOT headgroup model, SDSS, in the absence of aggregates. When the yields from reaction in the reference and micellar (or vesicular) solutions are the same, the nucleophile molarities in the green interfacial region (Box **A**) are assumed to be the same as those in the green reference solution (Box **B**).

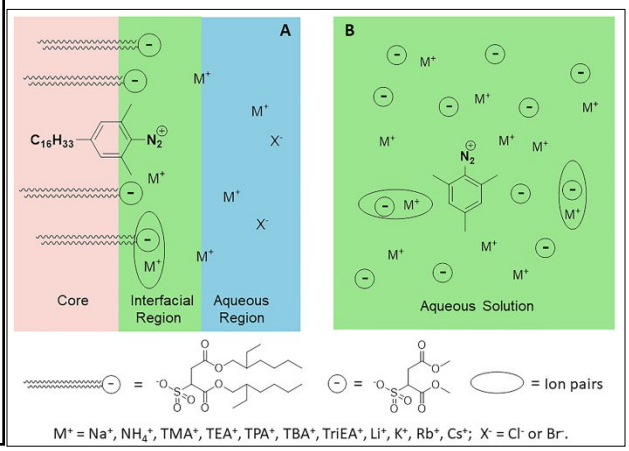

Table 1. Average hydrodynamic diameters, nm, for triplicate DLS measurements of AOT (15 mM) aggregates at 3, 7, 7.5, 30 and 50 mM of the salts listed in the

second and seventh columns at 28 °C. The salt concentrations in the second and sixth columns were obtained at their maximum concentrations shown in **Figure 3, 4** and **6**.

No.	Salt	Conc. /mM	Diameter /nm	Standard deviation	No.	Salt	Conc. /mM	Diameter /nm	Standard deviation
1	LiCl	50	88.8	0.1	10	NaBr	50	89.1	0.1
2	NaCl	50	97.8	0.0	11	NaSCN	50	104.8[a]	0.7
3	KCl	50	93.2	0.5	12	NaBenz	50	94.6[a]	0.5
4	RbCl	50	106.4	0.2	13	NaSal	50	118.2	0.7
5	CsCl	50	90.4	0.7	14	TMABr	50	72.7	0.3
6	$MgCl_2$	7	86.3	0.6	15	TEABr	50	295.8	2.4
7	$CaCl_2$	7.5	214.4	0.2	16	TPABr	50	252.2	0.5
8	$ZnCl_2$	7.5	79.0	0.4	17	TBABr	30	1111.3	8.4
9	$AlCl_3$	3	227.0	0.7	18	TriEABr	50	94.6	0.2
					19	NH_4Br	50	88.4	0.3

a. Our vesicle diameters, ca. 100 nm, for NaBenz and NaSal are considerably smaller than the ca. 280 nm estimated for these vesicles.[33] The reason is not known.

***Estimating interfacial AOT_m and H_2O_m molarities in AOT aggregates with added salts*.** **Table 2** lists representative results for the only two CT products observed by HPLC, 16-ArOH from interfacial water, and 16-ArS from reaction with AOT sulfonate headgroups from the reaction of ca. 6.1 x 10^{-5} M 16-ArN_2^+ in 15 mM AOT, 0-50 mM tetramethylammonium bromide, TMABr, [HBr] = 1 mM, at 28 °C. In general the AOT/16-ArN_2^+ ratio was ≥ 125/1 and we assume micelle perturbation by the probe was minimal. This temperature was used in all dediazoniation experiments because the microtubes in the thermal mixer failed to maintain a constant temperature of 25 °C for long periods (days) in our too warm labs. HBr (1 mM) was added to control solution acidity and to minimize the formation of byproducts, which was effective.[68] Included in **Table 2** are the average HPLC peak areas, observed and normalized product yields, and estimated interfacial molarities, M, in units of moles per liter of interfacial volume, of AOT headgroups, AOT_m, and water H_2O_m and their molar ratios, H_2O_m/AOT_m. The observed yields of %16-ArOH and %16-ArS were calculated from HPLC peak areas. Their calibration curves are listed

Table 2. HPLC average peak areas, observed and normalized (subscript N) product yields for dediazoniation reaction of 16-ArN_2^+ in solutions of 15 mM AOT in the present of 0-50 mM TMABr, estimated interfacial molarities of headgroup, AOT_m, water, H_2O_m, and their molar ratio, H_2O_m/ AOT_m, at 28°C. [HBr] = 1 mM.[a]

[TMABr] (mM)	Shaker[b]	Peak Areas (10^6μv•s)[c]		Observed Yields (%)			Normalized Yields (%)[d]		AOT_m[e] (M)	H_2O_m[e] (M)	H_2O_m /AOT_m[e]
		16-ArOH	16-ArS	16-ArOH	16-ArS	Total	16-$ArOH_N$	16-ArS_N			
0	Yes	5.29	0.75	87.2	8.9	96.2	90.7	9.3	1.06	44.65	42.2
0	No	5.21	0.77	85.8	9.1	94.9	90.4	9.6			
1	Yes	5.24	0.73	86.4	8.7	95.1	90.8	9.2	1.02	45.01	44.0
1	No	5.42	0.76	89.3	9.0	98.3	90.9	9.1			
5	Yes	5.20	0.81	85.8	9.6	95.4	89.9	10.1	1.11	44.19	40.0
5	No	5.31	0.79	87.4	9.4	96.8	90.3	9.7			
10	Yes	5.17	0.83	85.2	9.8	95.0	89.7	10.3	1.15	43.78	38.2
10	No	5.21	0.82	85.9	9.7	95.6	89.8	10.2			
13	Yes	5.06	0.85	83.4	10.1	93.5	89.2	10.8	1.19	43.37	36.5
13	No	5.22	0.85	86.0	10.1	96.1	89.5	10.5			
15	Yes	5.07	0.89	83.5	10.5	94.1	88.8	11.2	1.23	42.93	34.8
15	No	5.14	0.87	84.6	10.3	95.0	89.1	10.9			
20	Yes	4.84	0.88	79.8	10.5	90.3	88.4	11.6	1.31	42.22	32.3
20	No	4.98	0.92	82.0	10.9	93.0	88.2	11.8			
30	Yes	4.51	1.23	74.5	14.6	89.1	83.6	16.4	1.83	37.01	20.2
30	No	4.56	1.25	75.1	14.8	90.0	83.5	16.5			
50	Yes	4.42	1.33	72.9	15.8	88.7	82.2	17.8	1.99	35.46	17.8
50	No	4.41	1.34	72.7	15.9	88.6	82.0	18.0			

a. Reaction time ca. 48 hours. Prior to HPLC analysis, the product mixture was mixed with an equal volume of water. The final concentrations of 16-ArN_2^+ were ca. 6.1 x 10^{-5} M. **b**. The reaction tubes were either placed in a thermostated shaker or water bath. c. 100 μL sample injections. Peak areas are average of triplicate or duplicate injections. Eluting solvents: 65%MeOH/35%*i*-PrOH; Flow rate: 0.4 mL/min; Detector wavelength: 220 nm. d. Calculation of normalized yields ($_N$). %16-ArS_N = 100 (%16-ArS)/(%16-ArOH + %16-ArS); % 16-$ArOH_N$ = 100 (%16-ArOH)/(%16-ArOH + %16-ArS). e. For each solution composition, the estimated AOT_m and H_2O_m values were average results calculated from both experiments carried out with or without shaker.

in **Table S1**. **Table 2** also shows the results of a control experiment in which the chemical trapping reactions were carried out twice, with and without stirring (See **Experimental Section**). Delightfully, the two results were almost identical (the standard deviations were < 1%). This identity also supports our assumption that the solutions are in dynamic equilibrium. The calculated interfacial molarities are the average results from experiments with ca. $< 10^{-4}$ M 16-ArN_2^+ in micelles and vesicles.

The captions for **Figures 3**, **4**, and **5** give the equations for calculating headgroup interfacial molarities. Complete results for other alkyl ammonium organic salts listed in **Table 1** are given in the **ESI**, **Tables S2-S6.** Results for metal ion salts are also in the **ESI, Table S7-S20**. All these **Tables** contain the same type of information as listed in **Table 2**.

***Changes in H_2O_m and AOT_m values with added salts*.** **Figures 3, 4,** and **5** show the effects of added Na^+ and variable anion, a variety of metal ions with variable valences, and organic cations of variable size and structure, respectively. These figures are presented and discussed separately because they have underlying similarities in changes in interfacial molarities of AOT_m and H_2O_m with added salts, but also some marked differences with changes in cation size (organic) or valence (metal ions).

Figure 3 shows that for a series of Na^+ salts, NaY, only RSO_3^- headgroups and water trap 16-ArN_2^+ despite relatively large changes in size, hydrophobicity, and polarizability of their co-ions: Y = Cl^-. Br^-, SCN^-, benzoate, and salicylate. The calculated values of H_2O_m, AOT_m and H_2O_m/AOT_m, for all the salts show a nearly identical dependence on stoichiometric salt concentration within experimental error. These results are similar to those of NH_4^+ in **Figure 4**. The numerical results for the data in **Figure 3** are listed in **Table S8** and **Tables S16-19** in the **ESI**. No products with the anions, Y^-, were observed in the HPLC results indicating that anionic co-ions listed in the **Figure 3** do not form products with the probe in AOT interfaces. Prior results also show no specific interactions with interfacial co-ion components in AOT reverse micelles.[63] Perhaps because of the relatively low salt concentrations used here and/or because the anions are outside the interfacial region, or both, they do not form pairs with 16-ArN_2^+. The radial distributions of the probe and the anions might be determined by MD. Added bulk Na^+ ions exchange with interfacial Na^+ (an identity reaction) with increasing Na^+ molarity in the interfacial region, which also increases the extent of ion-pairing with RSO_3^-. Water is released from the interfacial region

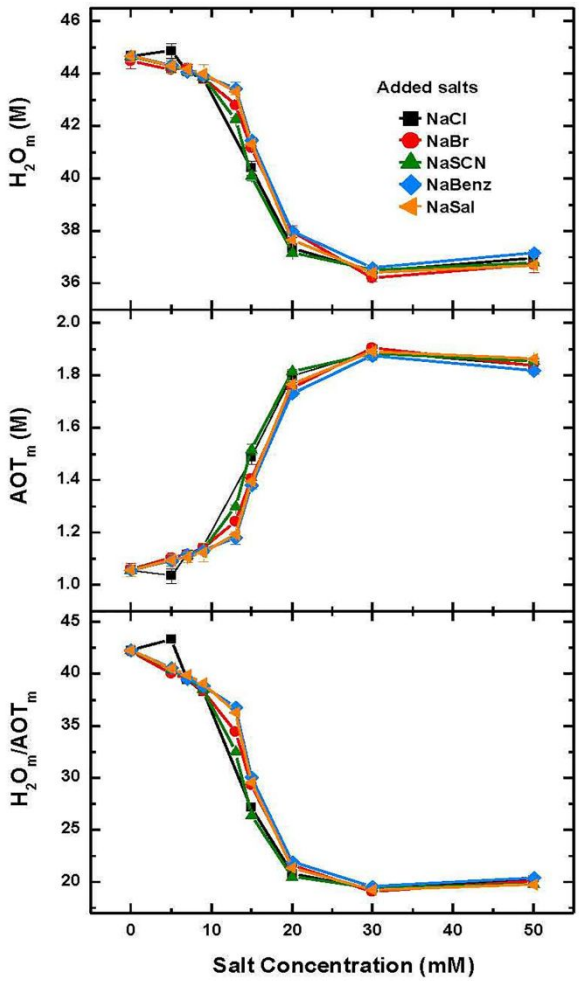

Figure 3. Changes in interfacial molarities of water, H_2O_m, headgroup, AOT_m, and their ratio, H_2O_m/AOT_m, with increasing stoichiometric concentrations of added NaY (Y= Cl, Br, SCN, benzoate, and salicylate) in 15 mM AOT solutions in the presence of 1 mM HBr at 28 °C. Lines are drawn to aid the eye. Error bars, which are about the size of the symbols, show the variation in data because for each concentration chemical trapping reactions were carried out twice, with stirring or not. Equations previously determined by carrying out dediazoniation reactions with 1-ArN_2^+ in SDSS aqueous reference solutions A) %16-ArS = 9.04 x AOT_m – 0.103 and B) %16-ArOH = 0.914 x H_2O_m + 49.7 were used to convert the product yields of 16-ArS and 16-ArOH into interfacial molarities of RSO_3^- headgroup and H_2O, respectively.[64]

and the process continues with added salt up to about 20 mM, when vesicle formation is complete and interfacial molarities of H_2O_m, headgroups, AOT_m, and their ratio, H_2O_m/AOT_m, are essentially constant—probably because vesicle bilayers cannot change size and shape as easily as micelles. The near identity of the results in **Figure 3** for all the salts shows that the values for the interfacial molarities of

Na^+ and H_2O are quite reproducible for the ions listed in **Figure 3** and the strong similarity of the vesicle diameters in **Table 1** for the salts in **Figure 3** supports this interpretation. Values of H_2O_m depend on the interfacial concentration of water molecules and its calculated molarity is from competitive reaction of 16-ArN_2^+ with RSO_3^-. However, the yield from reaction with RSO_3^- will increase with the concentration of added salt because more ion-pairs in the interfacial region will form with added salt, decrease hydration, and decrease the yield from reaction of 16-ArN_2^+ with headgroups. A decrease in interfacial water will, to some extent, permit tighter packing of charged headgroups and increase ion-pairing and this will affect interfacial molarities of RSO_3^- with added salt. Note that AOT_m approximately doubles between 0 to 50 mM added salt. However, although the number of free, unpaired, headgroups is uncertain, the results suggest that it is quite reproducible for each salt in **Figure 3**.

The shapes of the interfacial molarity-salt concentration profiles in **Figure 3** reappear often in **Figures 4** and **5**. H_2O_m decreases and AOT_m increases and their ratios change from about 40 H_2O_m/AOT_m when micelles are present ([salt] = 0 mM) to about 20 H_2O_m/AOT_m at the plateau from 20 to 50 mM added salt. This pattern looks different in **Figures 4** and **5**, in part because of differences in the Y-axis scales and because other changes are also occurring, e.g., phase separation for some cations.

Metal Cations. **Figure 4** shows chemical trapping results from the dediazoniation of 16-ArN_2^+ in 15 mM aqueous AOT solutions containing 0-50 mM metal cation chloride salts, 1 mM HCl at 28 ^oC and the same 16-ArN_2^+/probe ratios as in earlier experiments, $\geq$ 125/1. The metal ions of the added inorganic salts were monovalent, MCl (M = Li, Na, K, Rb, Cs), divalent, MCl_2 (M = Ca, Mg, Zn), or trivalent, $AlCl_3$. The concentration ranges for multivalent chloride salts are below 50 mM because these solutions precipitate above the highest listed salt concentrations. **Tables S7-S15** in the **ESI** list the numerical results and are analogous to **Table 2.** The solution ionic strengths are not the same at all metal ion molarities. The Cl^- concentrations for divalent or trivalent metal salts are double or triple those of the monovalent salts. Note that for monovalent salts, the increases in AOT_m (ca. 1-1.9 M) and concomitant decreases in H_2O_m, (ca. 45-36 M) and the H_2O_m/AOT_m ratio drops from ca. 44 to about 20 for most cations, which is similar to that for Na^+. Here there is a distinct dependence on cation type with Cs^+ having the biggest effect on H_2O_m and AOT_m and Li^+ the least effect, which is a measure of the

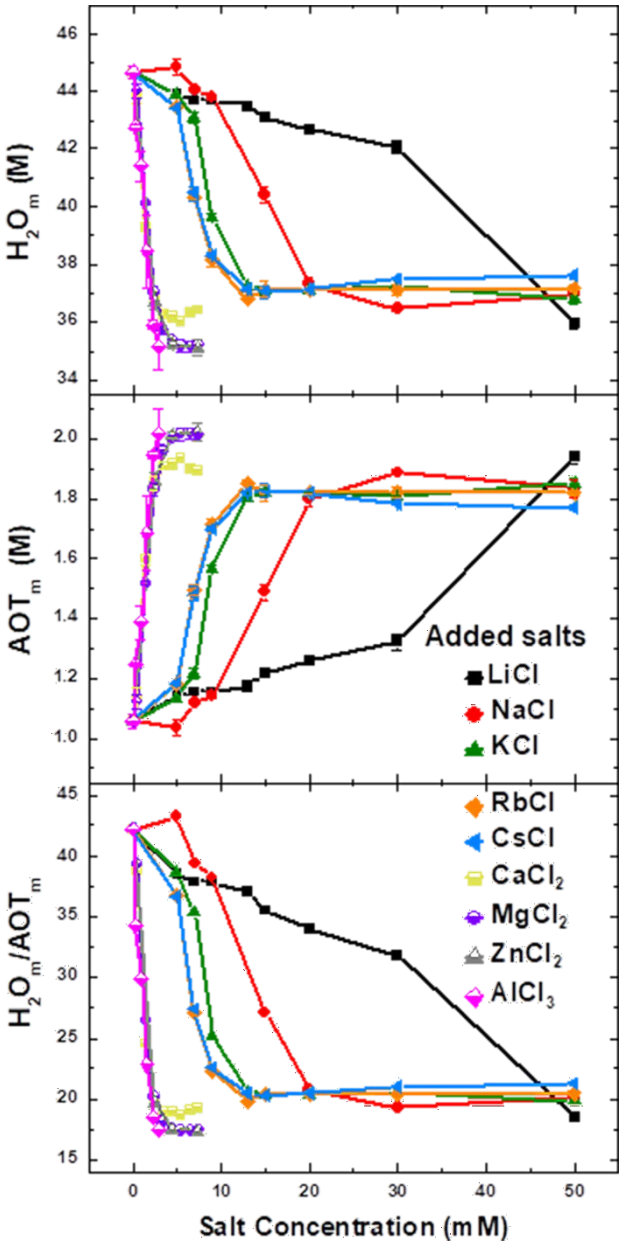

Figure 4. Changes in interfacial molarities of water, H_2O_m, headgroup, AOT_m, and their ratio, H_2O_m/ AOT_m, with increasing stoichiometric concentrations of added organic ammonium salts in 15 mM AOT solutions in the presence of 1 mM HBr at 28 °C. Lines are drawn to aid the eye. Error bars, which are very small, show the variabilities of the data because for each concentration chemical trapping reactions were carried out twice, with stirring or not. Equations previously determined by carrying out dediazoniation reactions with 1-ArN_2^+ in SDSS aqueous reference solutions A) %16-ArS = 9.04 x AOT_m – 0.103; and B) %16-ArOH = 0.914 x H_2O_m + 49.72 were used to convert the product yields of 16-ArS and 16-ArOH into interfacial molarities of AOT headgroup and water, respectively.[64]

counterion's ability to displace Na^+ ions from the micellar interface. The cations follow the order: $Cs^+ \approx Rb^+ \approx K^+ > Na^+ > Li^+$, which is consistent with the Hofmeister series. Much lower concentrations of multivalent cations are needed to induce interfacial dehydration and increase AOT_m, which occurs at the same solution concentration range（from 1.5 to 7.5 mM）as the solutions' physical appearance changes from clear to bluish and cloudy. The hydration changes in the interfacial region shown in **Figure 5** are similar to the results in **Figure 3**. Note that Ca^{2+} and Al^{3+} make vesicles about twice the size of the other divalent cations, **Table 1**.

Organic Cations. **Figure 5** shows the effect of added ternary and quaternary ammonium organic salts, R^+Br^-, from 0 to 50 mM at 28 °C in 15 mM AOT on interfacial H_2O_m, AOT_m, and H_2O_m/AOT_m molar ratios determined by CT. Transitions for cations that interact less strongly than Na^+ occur at higher added R^+Br^- mM and those that interact more strongly than Na^+ at lower added R^+Br^- mM. The results with TBA^+ have much greater changes that distort the appearance of the results compared to the other ions, which are qualitatively similar to those in **Figures 3** and **4**, but are squeezed together.

At 0 R^+Br^-, the only cation is Na^+ and the start points for all salts are the same, ca. 45 M, H_2O_m, ca. 1 M AOT_m, and ca. 42 M H_2O_m/AOT_m, **Figure 5**. For all added R^+Br^-, the values of H_2O_m, AOT_m, and H_2O_m/AOT_m follow sigmoidal curves downward or upward and reach plateaus similar to those in **Figures 3** and **4**. Between 0 to 50 mM added salt, the maximum decrease in H_2O_m is to ~ 35, $\Delta \approx 10$; the increase in AOT_m is to ~ 2, $\Delta \approx 1$; and the decrease in H_2O_m/AOT_m is to ~18, $\Delta \approx 24$. As the hydrophobicities of the salts increase, the concentration of added R^+Br^- versus salt concentration in each plot required to reach the plateau decreases: $TBA^+ < TPA^+ < TMA^+ \approx TEA^+$, i.e., the order follows a Hofmeister series based on decreasing cation hydrophobicity and size. The orders for NH_4^+ and $TriEA^+$ cations are reversed, probably because two effects contribute, hydrogen bonding and hydrophobicity. Their relative importance is not known.

The orders are most clearly illustrated in the H_2O_m/AOT_m against added R^+Br^- salt profiles. NH_4^+ and $TriEA^+$ reach the plateau regions about the same concentration as added Na^+, which indicates that the interactions of these cations with the AOT headgroups are about the same. The DLS results in **Table 1** show that TMA^+, NH_4^+, and $TriEA^+$ cations make small vesicles like those of Na^+, but TEA^+, TPA^+ and

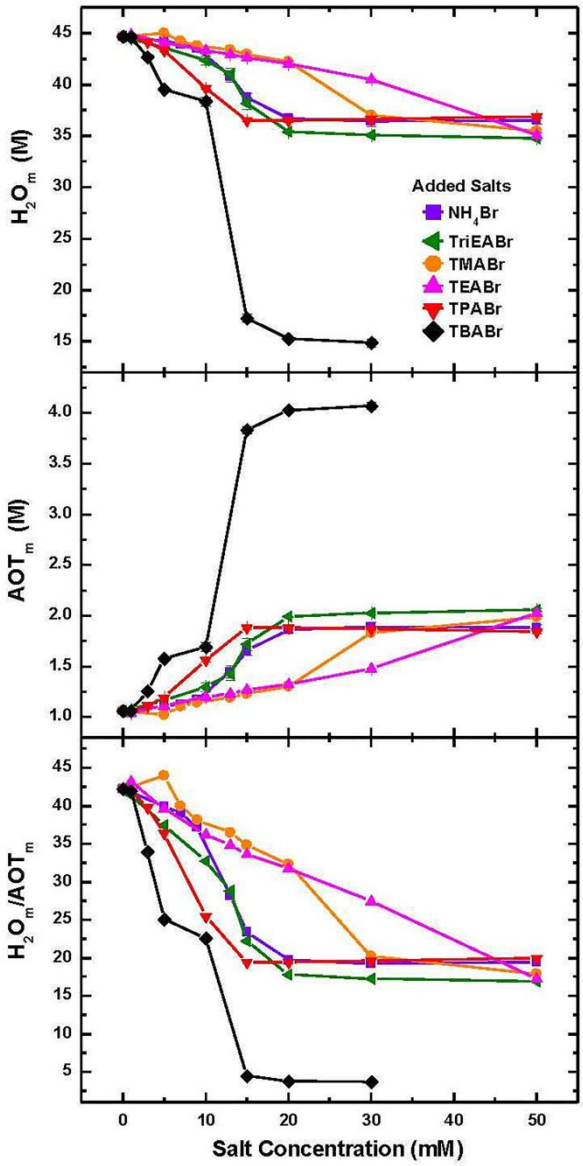

Figure 5. Changes in interfacial molarities of water, H_2O_m, headgroup, AOT_m, and their ratio, H_2O_m/AOT_m, with increasing stoichiometric concentrations of added organic salts in 15 mM AOT solutions in the presence of 1 mM HCl at 28 °C. Lines are drawn to aid the eye. Error bars show the variabilities of the data because for each concentration chemical trapping reactions were carried out twice, with stirring or not. TriEABr (green) is almost totally superimposable on NH4Br (purple). Equations previously determined by carrying out dediazoniation reactions with 1-ArN_2^+ in SDSS aqueous reference solutions A) %16-ArS = 9.04 x AOT_m – 0.103 and B) %16-ArOH = 0.914 x H_2O_m + 49.7 were used to convert the product yields of 16-ArS and 16-ArOH into interfacial molarities of AOT headgroup and water, respectively.[64]

TBA^+ make vesicles that are two to three larger and TBA^+ makes aggregates >10 times larger. These size increases are clearly related to the increasing hydrophobicities of the cations, but how they affect curvature on the endo and exo surfaces is not known.

All the solutions are optically transparent up to 50 mM added salt, except TBABr, which forms cloudy mixtures above 10 mM. TBABr has much larger changes in the interfacial headgroup and water molarities and their ratios. Addition of 30 mM TBABr decreases H_2O_m from 40 to 15 M, increases AOT_m from ca. 1 to 4 M and the H_2O_m/AOT_m, molar ratio drops from 42 to 4, a >10 fold decrease. The rate of change in interfacial molarities is greatest for TBA^+.

For TBA^+, initial dehydration is almost complete at about 10 mM added TBABr, **Figure 5**. Increasing TBA^+ up to 30 mM produces a dramatic change in interfacial composition, **Figure 5**. The H_2O_m/AOT_m ratio shows that about 42 water molecules hydrate the AOT headgroups and counterions in the interfacial region when only Na^+ is present. At 30 mM TBABr, the H_2O_m/AOT_m ratio has decreased to 5, a nearly 90% decrease in the amount of interfacial water. The physical appearance of the mixture also changes from clear bluish to an opaque white. At higher concentrations, e.g., to 50 mM, precipitates formed.

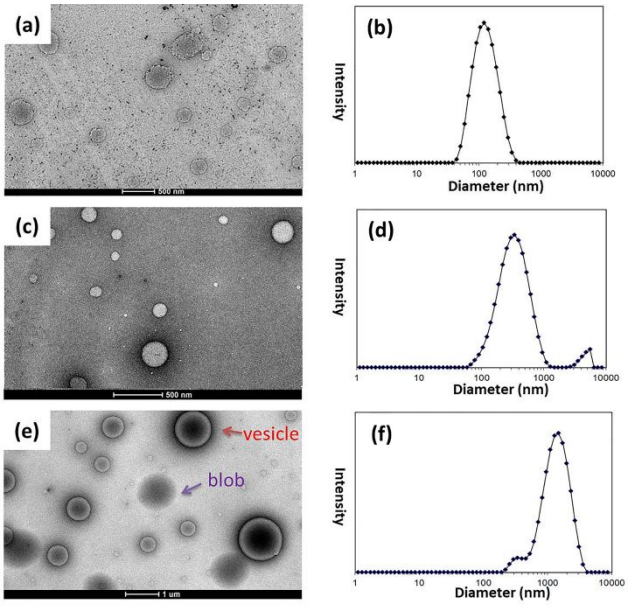

Figure 6. TEM images and DLS data of 15 mM AOT aqueous solutions with added 10 mM TBABr (a and b), 15 mM TBABr (c and d), 30 mM TBABr (e and f).

TEM and DLS Studies, **Figure 6**, show that the dehydration and changes in physical appearance are caused by an increase of the average diameter of aggregates from ~100 nm to ~1.1 μm. At 30 mM added TBA^+, large amorphous spherical "blobs" appear in the DLS images that we cannot identify unambiguously, but appear to coexist with vesicles, for example, and the system may not be at dynamic equilibrium. One possibility is that the blobs are formed by secondary aggregation of smaller micelles of the strongly dehydrated $AOT^-•TBA^+$

pairs forming aggregates in which the alkyl chains of TBA^+ bind smaller micelles together. Large structures formed by amphiphilic molecules containing β-cyclodextrin and ferrocene as linkers have been reported.[72-74]

Modeling Counterion Binding and Water within Association Colloid Interfaces. As noted earlier, the specific ion effects that govern cation association to micellar interfacial regions within the AOT aggregates as they change from micelles to vesicles depend on multiple interactions. **Scheme 1** illustrates some of the important equilibria that may influence association interactions in the interfacial pseudophase. They are not easy to quantify. The hydrophobic effect is the most well-known and probably the least important in directly affecting interfacial interactions once the aggregates are formed. The extent of *ion-pairing* depends on the strength of the interaction of the RSO_3^- headgroup and the Na^+ or other specific cations that have different interactions. Collins has discussed these interactions in some detail and our results are consistent with his interpretation.[38] The extent of interfacial coverage by an added cation depends on its affinity for RSO_3^- compared to Na^+, and large more polarizable cations should associate more strongly and be more difficult to displace. The ion-pair will release an uncertain number of water molecules because the ion-pair is a polar, but charge neutral complex and its hydration demand is less than that of free ions. Ion exchange is an established concept for describing the competition between two counterions in micellar solutions,[70] but in the past, specific headgroup-counterion pairing was not considered part of the process.

Scheme 1

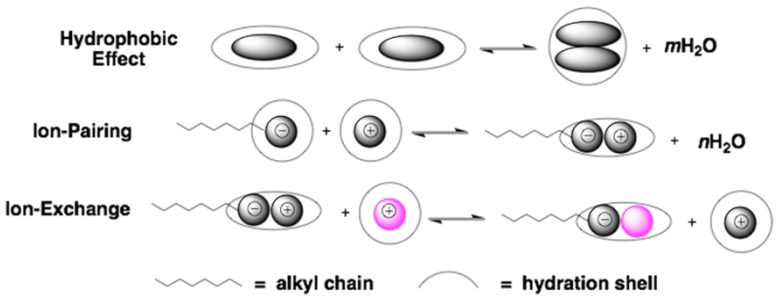

The top equilibrium in **Scheme 1** illustrates the *Hydrophobic Effect* in aqueous solution, in this example equilibrium dimerization of shaded hydrophobic ovals and the release of water with an increase water disorder and entropy.[75] A hydrophobic dimer may phase separate, but if the ovals are joined to charged headgroups to make ionic surfactants, then 50-100 of them may aggregate spontaneously into a micelle releasing much of the water associated with the hydrocarbon tails. The *Ion-Pairing* equilibrium, **Scheme 1**, middle, shows headgroup

and counterion pairing in the interfacial region of these aggregates or with headgroup models in bulk solution. In the interfacial region, hydrated free ions form polar and less hydrated, formally neutral headgroup-counterion pairs. They are also formed by short-chain analogs at high salt concentrations in aqueous solution. An unknown amount of water is released and leaves the interfacial region. The *Ion-Exchange* equilibrium, **Scheme 1**, bottom, also occurs in both the interfacial and aqueous regions, but only in the interfacial region does it affect micellar properties directly because of the change in specific interactions between the headgroup and the counterion and the much higher concentration of counterions within the micellar interfacial region. Because the hydration demand by ion-pairs is less than that of unpaired ions, the equilibrium shifts in favor to the right because of stronger association. All three equilibria may release water into the surrounded bulk solution, but the amount depends on the strength of the hydration interactions and specific ion interactions that determine the positions of equilibrium. The hydrophobic effect is primarily responsible for micelle formation. The ion exchange equilibria is responsible for the counterion composition of the micellar surface and the ion-pairing equilibria for specific ion association and release of interfacial water.

Scheme 2 illustrates a small section of a spherical micelle in dynamic equilibrium with a section of a vesicle bilayer. Addition of salts to AOT micellar solutions changes H_2O_m, $AOT_{m,}$ and H_2O_m/AOT_m that are sensitive to changes in cation size and charge for monovalent cations. Adding salt increases AOT_m from about 1 to 2 M with accompanying decreases in H_2O_m until it reaches the H_2O_m/AOT_m ratios for vesicles and plateaus. With few exceptions: the interfacial compositions of 20-25 mM to 50 mM added salt in **Figures 3**, **4** and **5**, are essentially constant, H_2O_m ca. 35-36 M, AOT_m ca. 2 M, and the H_2O_m/AOT_m ratio of about 20.

The results in **Figures 3, 4,** and **5**, provide straightforward evidence for why micelles undergo shape changes with added M^{n+}. As MX_n concentration increases the number of ion-pairs in the interfacial region increases and the volume of interfacial water decreases significantly. Loss of interfacial water leads to tighter interfacial headgroup and counterion packing, i.e., an increase in the packing parameter,[5] and the formation of aggregates with lower degrees of interfacial curvature such as rods and vesicles. That is, surfactant headgroup counterion pairing and simultaneous dehydration in the interfacial region, increases interfacial packing. Therefore, different ion-pairing abilities of different added counterions with the headgroups produce the

ion-specific effects on the micelle-to-vesicle transition.[41, 43, 44] Other evidence includes the dehydration of cationic micelles at their sphere-to-rod transitions.[70]

The initial and plateau values of the interfacial molarities are the same as in **Figures 3. 4 & 5** and the transition concentrations increase with increasing cation size, with Li^+ being the least effective ion. The monovalent cations produce vesicles of similar size, ca. 100 nm and the di and tri cations results are essentially the same, except that Ca^{2+} and Al^{3+} cations produce larger vesicles and phase separation. In the plateau regions, 20 to 50 mM added salt, the interfacial compositions become independent of added cation type and concentration, except for TBABr. This indicates that for AOT, the headgroup, counterion and water form vesicles of similar shape and size. Other aggregate structures, of course, are possible depending on surfactant size and shape, counterion type, headgroup structure, or the presence of oil, not used in these experiments.

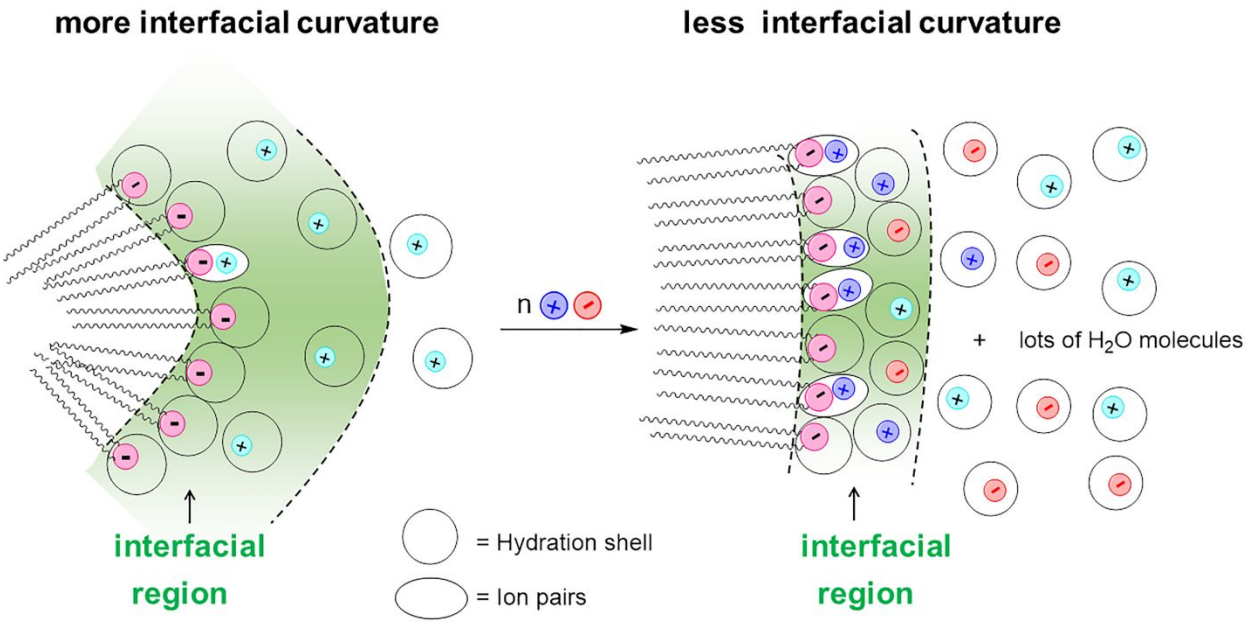

Scheme 2. Added salt, MX_n, affect on the interfacial composition of AOT micelles (left) and vesicles (right). The exo wall of the vesicle is illustrated on the right after and equilibrium has been reached. The endo wall is assumed to look the same. The figure illustrates the effect of salt addition on water loss, the fraction of headgroup-counterion pairs, tighter packing, the decrease in interfacial volume and interfacial thickness, and the increase in interfacial headgroup and counterion molarity and decrease in interfacial water.

The results in **Figures 3, 4,** and **5**, provide straightforward evidence for why micelles undergo shape changes with added M^{n+}. As MX_n concentration increases, the number of ion-pairs in the interfacial region increases and the volume of interfacial water decreases significantly. Loss of interfacial water leads to tighter interfacial headgroup and counterion packing, i.e., an increase in the packing parameter,[5] and the formation of aggregates with lower degrees of interfacial curvature such as rods and vesicles. That is, surfactant headgroup counterion pairing and simultaneous dehydration in the interfacial region, increases interfacial packing. Therefore, different ion-pairing abilities of different added counterions with the headgroups produce the ion-specific effects on the micelle-to-vesicle transition.[41, 43, 44] Other evidence includes the dehydration of cationic micelles at their sphere-to-rod transitions.[70]

Specific Ion-Pairing/Hydration Model and the Hofmeister Series. The amount of water released on ion-pair formation in the interfacial regions depends on the fraction of tight and water separated pairs, and the free energies of hydration of the headgroup and counterion, **Scheme 2**. The transitions occur when interfacial headgroup, counterion, water packing increases sufficiently to permit spherical structure to become "flatter," because the headgroup sizes are smaller, that is, from spheres, to rods, to vesicles, to lamellar structures. Interfacial counterion molarities are generally high, 1-3 M,[65] but there are a number of estimates of interfacial molarities for micelles in the presence and absence of added salt and structural transitions leading to an increase in the packing parameter.[30, 65, 76-78] As water molecules diffuse into the surrounding aqueous region the solution entropy increases because water of hydration has a lower entropy than bulk water.[75] This entropy increase may also contribute to the driving force for micelle formation and structural transitions. Note that ion-pair formation in the interfacial region leads to release of water to the aqueous region and a decrease in interfacial volume, but ion-pairing in aqueous pseudophase releases water, but no significant change in the volume of the aqueous pseudophase.

Taken together, **Schemes 1** and **2** are a tentative description of the equilibria for ion-pair formation between one AOT headgroup, one counter cation and water interacting in the interfacial region, In a different experiment with larger cation with the same interactions, the equilibrium constant for pairing would increase, the hydration of the larger ion would probably be smaller and the paired ions would be dehydrated to some extent. At equilibrium, the second cation would have a larger effect than the first cation.

A third, or fourth, or fifth monovalent cations that have progressively larger sizes would increase the equilibrium constant progressively. For a series of cations with a single headgroup, in which the equilibrium constant increases with some cation parameter might generate a Hofmeister series that correlates with ion, size assuming other interactions remain approximately constant. The actual effect of a particular cation will depend on the number and strength of specific interactions contributing to the overall strengths of the ion-pairing interactions. The same logic holds for anions interacting with cationic surfactant headgroups and counter anions in micelles.

Figures 3-5 shows that the Specific Ion-Pair/Hydration model qualitatively accounts for the following observations with changing cation type:

- When the cation is Na^+, the changing of the anion had no effect on H_2O_m, AOT_m, and H_2O_m/AOT_m, **Figure 3**. This is consistent with Na^+ and RSO_3^- in the micellar interface forming tight ion-pairs and that added co-anions cannot compete with RSO_3^- for 16-ArN_2^+, including the more hydrophobic anions.
- For monovalent cations, **Figure 4**, displacement of Na^+ by M^+ on the H_2O_m/AOT_m ratio correlates well with cation size for the monovalent ions, but the di- and trivalent ions displace Na^+ completely at low concentrations and precipitate the surfactant above about 8 mM salt indicating that multivalent cations have stronger interactions with RSO_3^- than monovalent cations.
- For displacement of Na^+ by R_4N^+ alkyl ammonium cations, **Figure 5**, the more hydrophobic the cation the more effective it is at displacing interfacial water. When R = 4, the surfactant phase separates.

Thus, when only one ion property or a pair of properties change at a time, the order follows a Hofmeister series. However, if for a variety of cations were used with different properties or mixtures of properties, e.g., small size, but high polarizability, such correlations with one property may not hold.

Conclusions. Our result for AOT micelles demonstrate that salt induced micelle-to-vesicle transitions are sensitive to cation, but not anion type and are accompanied by a marked concurrent decreases in interfacial water molarity and increases in interfacial headgroup molarity. The results are consistent with the small-angle neutron scattering (SANS) measurements of Ismail et al.[8, 41, 57, 58] that demonstrate that there is a specific cation effect on the micelle-to-vesicle transitions of 15 mM aqueous AOT solutions in the presence of various salts.[41] Finally, the results show that interfacial dehydration is

required for the ion-specific micelle-to-vesicle transitions and that they are consistent with the Specific Ion-Pair/Hydration model.

Experimental Section

General methods. HPLC measurements were performed on a Perkin-Elmer Series 200 equipped with a UV/Vis detector, a Varian Microsorb MV C18 column (length, 25 cm; particle size, 5 m), and a computer-controlled Perkin-Elmer 600 Series Interface. Conditions for product separation on the HPLC were: a 65% MeOH/35% *i*-PrOH (v/v) mobile phase; flow rate = 0.4 mL/min; detector wavelength λ = 220 nm; and the injection volume was 100 μL. ^{1}H NMR spectra were recorded on Varian VNMRS 500 MHz spectrometer. The temperature of the chemical trapping experiments was maintained by a Haake A10 circulation bath or a Fisher scientific microtube thermal mixer.

Materials. All aqueous solutions were prepared from water that was distilled, passed over activated carbon, an ion exchange resin and then redistilled. MeOH and *i*-PrOH were of the highest commercially available reagent grade. AOT, which comes with a Na^+ counterion (Sigma, 99%). were used as received. All additives, TMABr (Sigma, 98%), TEABr (TCI America, 98%), TPABr (TCI America, 98%), TBABr (TCI America, 98%), TriEABr (Alfa Aesar, 98%), NH_4Br (Sigma, 99%), LiCl (Sigma, 99%), NaCl (Alfa Aesar, 99%), KCl (Sigma, 99%), RbCl (Sigma, 99%), CsCl (Sigma, 99.9%), $MgCl_2$ (Sigma, 98%), $CaCl_2$ (Sigma, 97%), $ZnCl_2$ (Sigma, 97%), $AlCl_3$ (Fluka, 99%), NaBr (Sigma, 99%), sodium salicylate NaSal (Alfa Aesar, 99%), sodium benzoate NaBenz (Alfa Aesar, 99%), NaSCN (Sigma, 98%) were used as received. 16-ArOH and 16-ArS was prepared by established procedure.[62, 64]

Chemical trapping with 16-ArN_2^+ in aqueous AOT/salt solutions. The reaction was initiated by adding 50 μL freshly prepared stock solutions of 16-ArN_2BF_4 dissolved in ice-cold MeCN to 5 mL of the aqueous mixture of 15 mM AOT and added salts of the required concentrations, 1 mM HX, and a final probe concentration of 1.1-1.3 x 10^{-4} M. 1 mL of each reaction solution was transferred to a microtube, and was shaken and thermostated at 28 ^{o}C in a Fisher scientific microtube thermal mixer for 2 days. The remaining of each solution was thermostated at 28 ^{o}C in a water bath for 2 days. Samples with a bluish appearance are designated as containing large aggregates such as vesicles and giant micelles. The

physical appearance of the mixtures are consistent with literature.[41] Prior to HPLC analysis, the product mixtures were mixed with an equal volume of water. Percent yields were obtained from average values of peak areas from triplicate or duplicate injections with the appropriate calibration curves. Interfacial molarities of counterions and water were obtained percent yields of the products from reaction of 16-ArN_2^+ and water and $RSO3^-$ group on AOT. The equations describing the relationships between water and SDSS molarity was published earlier from product yields for the reaction of 1-ArN_2^+ with H_2O and with SDSS in the absence of added AOT.[64] The equations in units of moles per liter are:

$$\%1\text{-ArOH} = 0.914[H_2O] + 49.72 \quad (1)$$

$$\%1\text{-ArS} = 9.936[\text{SDSS}] + 0.103 \quad (2)$$

Applying the assumption that when the yields are the same in bulk solution for the SDSS and water and in the micellar interface for AOT and water, then the molarities in bulk water and the interfacial region are the same and:

$$\%16\text{-ArOH} = 0.914 \bullet H_2O_m + 49.72 \quad (3)$$

$$\%16\text{-ArS} = 9.936 \bullet AOT_m + 0.103 \quad (4)$$

All values of AOT_m and H_2O_m for figures in the manuscript and **ESI** were obtained using these two equations.

Transmission electron microscopy (TEM) observations. Negatively stained TEM micrographs were obtained using a Tecnai G^2 F20 TWIN Transmission electron microscope. One drop of each prepared solution was placed on a carbon-coated copper grid (300 mesh), and the excess liquid was absorbed using filter paper. One drop of 1.5% uranyl acetate aqueous solution was then added to the sample grid.

Dynamic light scattering (DLS) measurements. DLS measurements were carried out using a Malvern Instrument Zetasizer Nano equipped with a 22 mW He-Ne laser operating at a wavelength of 632.8 nm. The scattering angle was 173°. The samples were thermostated at 28 °C prior to and during measurements. Each sample was measured by three times. The distributions of diffusion coefficients of the solutes were obtained by analyzing the correlation function of scattering data via the CONTIN method. The apparent equivalent hydrodynamic diameters were therefore determined according to the

Stokes-Einstein equation. At the maximum concentration of each salt listed in Table 1, the integration of the main peak was greater than 98%. The hydrodynamic diameters reported in Table 1 were the peak values of the main peaks in the DLS graphs.

Acknowledgements The authors gratefully acknowledge support for this work by the National Key R&D Program of China (2017YFB0308701), National Science Foundation (NSF-ICC 1124776), the National Natural Science Foundation of China (21676003), the Beijing Municipal Science and Technology Project (D17110500190000), and the Beijing Technology and Business University Youth Scholars Fund (PXM2018_014213_000033). C.L. thanks Jiahui Xu for assistance with experiments.

References

1. M. J. Rosen, *Surfactants and interfacial phenomena*, John Wiley & Sons, New York, 2004.
2. D. F. Evans and H. Wennerström, *The colloidal domain: where physics, chemistry, biology, and technology meet*, VCH Publishers, New York, 1994.
3. B. Kronberg and B. Lindman, *Surfactants and polymers in aqueous solution*, John Wiley & Sons Ltd., Chichester, 1998.
4. K. L. Mittal and D. O. Shah, *Adsorption and aggregation of surfactants in solution*, CRC Press, Raton, 2003.
5. B. W. Ninham and P. Lo Nostro, *Molecular forces and self assembly: in colloid, nano sciences and biology*, Cambridge University Press, Cambridge, 2010.
6. N. Vlachy, B. Jagoda-Cwiklik, R. Vácha, D. Touraud, P. Jungwirth and W. Kunz, *Adv. Colloid Interface Sci.*, 2009, **146**, 42-47.
7. M. T. Yatcilla, K. L. Herrington, L. L. Brasher, E. W. Kaler, S. Chiruvolu and J. A. Zasadzinski, *J. Phys. Chem.*, 1996, **100**, 5874-5879.
8. J. Dey, J. Bhattacharjee, P. Hassan, V. Aswal, S. Das and K. Ismail, *Langmuir*, 2010, **26**, 15802-15806.
9. J. H. Fendler, *Chem. Rev.*, 1987, **87**, 877-899.
10. W. Kunz, J. Henle and B. W. Ninham, *Curr. Opin. Colloid Interface Sci.*, 2004, **9**, 19-37.
11. W. Kunz, P. Lo Nostro and B. W. Ninham, *Curr. Opin. Colloid Interface Sci.*, 2004, **9**, 1-18.
12. W. Kunz, *Curr. Opin. Colloid Interface Sci.*, 2010, **15**, 34-39.
13. J. Diamond and E. Wright, *Annu. Rev. Physiol.*, 1969, **31**, 581-646.
14. M. Cacace, E. Landau and J. Ramsden, *Q. Rev. Biophys.*, 1997, **30**, 241-277.
15. B. W. Ninham and V. Yaminsky, *Langmuir*, 1997, **13**, 2097-2108.
16. B. Jonsson, *Surfactants and polymers in aqueous solution*, John Wiley & Sons, Hoboken, 1998.
17. M. Boström, D. Williams and B. Ninham, *Phys. Rev. Lett.*, 2001, **87**, 168103.
18. P. Jungwirth and P. S. Cremer, *Nat. Chem.*, 2014, **6**, 261-263.
19. H. I. Okur, J. Hladílková, K. B. Rembert, Y. Cho, J. Heyda, J. Dzubiella, P. S. Cremer and P. Jungwirth, *J. Phys. Chem. B*, 2017, **121**, 1997-2014.
20. J. Heyda, J. Pokorná, L. Vrbka, R. Vácha, B. Jagodacwiklik, J. Konvalinka, P. Jungwirth and J. Vondrásek,

Phys. Chem. Chem. Phys., 2009, **11**, 7599-7604.
21. B. Hess, N. F. A. V. D. Vegt and K. A. Dill, *Proc. Natl. Acad. Sci. U. S. A.*, 2009, **106**, 13296-13300.
22. F. Hofmeister, *Naunyn-Schmiedeberg's Arch. Pharmacol.*, 1888, **25**, 1-30.
23. K. Kurihara, M. Tamura, K.-i. Shohda, T. Toyota, K. Suzuki and T. Sugawara, *Nat. Chem.*, 2011, **3**, 775-781.
24. K. Kurihara, Y. Okura, M. Matsuo, T. Toyota, K. Suzuki and T. Sugawara, *Nat. Commun.*, 2015, **6**, 8352.
25. Y. Elani, R. V. Law and O. Ces, *Nat. Commun.*, 2014, **5**, 5305.
26. G. Cevc, *Adv. Drug Delivery Rev.*, 2004, **56**, 675-711.
27. M. L. Immordino, F. Dosio and L. Cattel, *Int. J. Nanomed.*, 2006, **1**, 297.
28. J. Liu, Y. Jiang, Y. Cui, C. Xu, X. Ji and Y. Luan, *Int. J. Pharm.*, 2014, **473**, 560-571.
29. F. Liebig, R. Henning, R. M. Sarhan, C. Prietzel, M. Bargheer and J. Koetz, *Nanotechnology*, 2018, **29**, 185603.
30. N. F. Van Der Vegt, K. Haldrup, S. Roke, J. Zheng, M. Lund and H. J. Bakker, *Chem. Rev.*, 2016, **116**, 7626-7641.
31. K. Schweighofer and I. Benjamin, *The Journal of Chemical Physics*, 2000, **112**, 1474-1482.
32. E. Leontidis, *Curr. Opin. Colloid Interface Sci.*, 2016, **23**, 100-109.
33. U. Thapa, D. Ray, J. Dey, N. Sultana, V. Aswal and K. Ismail, *RSC Adv.*, 2015, **5**, 45956-45964.
34. Y. Zhang and P. S. Cremer, *Curr. Opin. Chem. Biol.*, 2006, **10**, 658-663.
35. F. S. Lima, M. F. Andrade, L. Mortara, L. G. Dias, I. M. Cuccovia and H. Chaimovich, *Phys. Chem. Chem. Phys.*, 2017, **19**, 30658-30666.
36. N. Vlachy, M. Drechsler, J.-M. Verbavatz, D. Touraud and W. Kunz, *J. Colloid Interface Sci.*, 2008, **319**, 542-548.
37. P. Lo Nostro and B. W. Ninham, *Chem. Rev.*, 2012, **112**, 2286-2322.
38. K. D. Collins, *Biophysical Journal*, 1997, **72**, 65-76.
39. S. Manet, Y. Karpichev, D. Bassani, R. Kiagus-Ahmad and R. Oda, *Langmuir*, 2010, **26**, 10645-10656.
40. A. Ohta, S. Nakashima, H. Matsuyanagi, T. Asakawa and S. Miyagishi, *Colloid and Polymer Science*, 2003, **282**, 162-169.
41. U. Thapa, J. Dey, S. Kumar, P. Hassan, V. Aswal and K. Ismail, *Soft Matter*, 2013, **9**, 11225-11232.
42. L. Medda, C. Carucci, D. F. Parsons, B. W. Ninham, M. Monduzzi and A. Salis, *Langmuir*, 2013, **29**, 15350-15358.
43. N. Vlachy, M. Drechsler, J. M. Verbavatz, D. Touraud and W. Kunz, *J. Colloid Interface Sci.*, 2008, **319**, 542.
44. A. Renoncourt, N. Vlachy, P. Bauduin, M. Drechsler, D. Touraud, J.M. Verbavatz, M. Dubois, W. Kunz and B. W. Ninham, *Langmuir*, 2007, **23**, 2376-2381.
45. H. Kawasaki, R. Imahayashi and H. Maeda, *Langmuir*, 2002, **18**, 8358-8363.
46. K. Horbaschek, H. Hoffmann and C. Thunig, *J. Colloid Interface Sci.*, 1998, **206**, 439-456.
47. K. D. Farquhar, M. Misran, B. H. Robinson, D. C. Steytler, P. Morini, P. R. Garrett and J. F. Holzwarth, *J. Phys.: Condens. Matter*, 1996, **8**, 9397.
48. E. W. Kaler, A. K. Murthy, B. E. Rodriguez and J. A. Zasadzinski, *Science*, 1989, **245**, 1371-1374.
49. K. L. Herrington, E. W. Kaler, D. D. Miller, J. A. Zasadzinski and S. Chiruvolu, *J. Phys. Chem.*, 1993, **97**, 13792-13802.
50. Y. Xia, I. Goldmints, P. W. Johnson, T. A. Hatton and A. Bose, *Langmuir*, 2002, **18**, 3822-3828.
51. J. J. Silber, A. Biasutti, E. Abuin and E. Lissi, *Advances in Colloid and Interface Science*, 1999, **82**, 189-252.

52. M. A. Luna, N. M. Correa, J. J. Silber, R. D. Falcone and F. Moyano, *J. Phys. Org. Chem.*, 2016, **29**, 580-585.
53. K. Fontell, *J. Colloid Interface Sci.*, 1973, **44**, 318-329.
54. B. Balinov, U. Olsson and O. Soederman, *J. Phys. Chem.*, 1991, **95**, 5931-5936.
55. M. Skouri, J. Marignan and R. May, *Colloid and Polymer Science*, 1991, **269**, 929-937.
56. I. Grillo, E. Kats and A. Muratov, *Langmuir*, 2003, **19**, 4573-4581.
57. I. Umlong and K. Ismail, *J. Colloid Interface Sci.*, 2005, **291**, 529-536.
58. J. Dey, U. Thapa and K. Ismail, *J. Colloid Interface Sci.*, 2012, **367**, 305-310.
59. L. S. Romsted, C. A. Bunton and J. Yao, *Curr. Opin. Colloid Interface Sci.*, 1997, **2**, 622-628.
60. L. S. Romsted and C. Bravo-Díaz, *Curr. Opin. Colloid Interface Sci.*, 2013, **18**, 3-14.
61. C. A. Bunton, Y.-S. Hong and L. S. Romsted, in *Solution Behavior of Surfactants*, eds. K. L. Mittal and E. J. Fendler, Plenum Press, New York, 1982, vol. 2, pp. 1137-1155.
62. A. Chaudhuri, J. A. Loughlin, L. S. Romsted and J. Yao, *J. Am. Chem. Soc.*, 1993, **115**, 8351-8351.
63. Iolanda M. Cuccovia, Augusto AgostinhoNeto, Caio M. A. Wendel, Hernan Chaimovich and L. S. Romsted, *Langmuir*, 1997, **13**, 5032-5035.
64. G. V. Srilakshmi and A. Chaudhuri, *Chem. - Eur. J.*, 2015, **6**, 2847-2853.
65. L. S. Romsted, *Langmuir*, 2007, **23**, 414-424.
66. A. A. Dar, L. S. Romsted, N. Nazir, Y. Zhang, X. Gao, Q. Gu and C. Liu, *Phys. Chem. Chem. Phys.*, 2017, **19**, 23747-23761.
67. I. M. Cuccovia, F. da Silva Lima and H. Chaimovich, *Biophys. Rev.*, 2017, **9**, 617-631.
68. A. A. Dar, C. Bravo-Diaz, N. Nazir and L. S. Romsted, *Curr. Opin. Colloid Interface Sci.*, 2017, **32**, 84-93.
69. Y. Geng and L. S. Romsted, *J. Phys. Chem. B*, 2005, **109**, 23629-23637.
70. Y. Geng, L. S. Romsted and F. Menger, *J. Am. Chem. Soc.*, 2006, **128**, 492-501.
71. A. Albert and E. P. Serjeant, *Ionization constants of acids and bases: a laboratory manual*, Methuen, 1962.
72. L. Zhao, S. Hao, Q. Zhai, H. Guo, B. Xu and H. Fan, *Soft matter*, 2017, **13**, 3099-3106.
73. Y. Bai, X.-d. Fan, H. Yao, Z. Yang, T.-t. Liu, H.-t. Zhang, W.-b. Zhang and W. Tian, *J. Phys. Chem. B*, 2015, **119**, 11893-11899.
74. C. Feng, G. Lu, Y. Li and X. Huang, *Langmuir*, 2013, **29**, 10922-10931.
75. C. Tanford, *The hydrophobic effect: formation of micelles and biological membranes 2d ed*, J. Wiley., New York, 1980.
76. B. P. Regler, T. J. Emge, J. J. Elliott, R. R. Sauers, J. A. Potenza and L. S. Romsted, *J. Phys. Chem. B*, 2007, **111**, 13668-13674.
77. L. S. Romsted, in *Recent Trends in Surface and Colloid Science*, ed. B. Paul, World Scientific, Hackensack, 2012, pp. 171-198.
78. L. S. Romsted, in *Encyclopedia of Supramolecular Chemistry: From Molecules to Nanomaterials*, eds. P. Gale and J. Steed, John Wiley & Sons, New York, 2012, vol. 1, pp. 181-203.

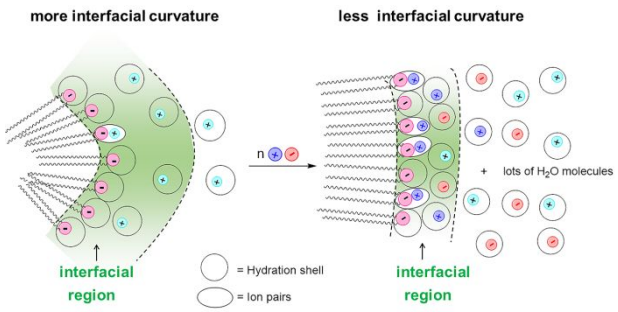

Added salts induce micelle-to-vesicle transitions at specific cation concentrations in Hofmeister order by forming polar headgroup-counterion pairs that release water.

Table of Contents Graphic, Max 8 cm (3.14”) by 4 cm (1.57”).

Draft Caption, 20 words